

A practical approach to assessing the induced voltage in signaling cables of the electrified transit systems

Praktyczne podejście do oceny indukowanego napięcia w przewodach sygnałowych zelektryfikowanych systemów tranzytowych

Abstract. *Electromagnetic Compatibility (EMC) is an essential requirement for every electrified transit system project. It is achieved by a complex approach of planning, design management and verification. One of the many important aspects of a transit system EMC is calculation and verification of the effects the noisy cables, usually power dc or ac, have upon victim cables, usually signal wires, run alongside system power cables in cable trays and conduits of the duct banks. This paper develops an approach to analyzing those effects for various geometrical relations between the noisy and victim wires.*

Streszczenie. *Kompatybilność elektromagnetyczna (EMC) jest zasadniczym wymaganiem dla każdego projektu zelektryfikowanego systemu tranzytowego. Kompatybilność osiąga się poprzez kompleksowe podejście do planowania, zarządzania projektowaniem i weryfikacji. Jednym z wielu ważnych aspektów EMC systemu tranzytowego jest obliczenie i weryfikacja wpływu kabli zakłócających, zazwyczaj mocy prądu stałego lub prądu przemiennego, na kable małej mocy, zwykle przewody sygnałowe, biegnące wzdłuż kabli zasilających systemu w korytkach kablowych lub kanałach przewodów. W artykule omówiono podejście i wzory do obliczania tych efektów dla różnych relacji geometrycznych pomiędzy kablem zakłócającym a przewodami sygnałowymi.*

Keywords: EMC, induced voltage, magnetic vector potential, touch potential

Słowa kluczowe: EMC, napięcie indukowane, potencjał wektorowy, napięcie dotykowe

Introduction

Electromagnetic Interference (EMI) is a phenomenon inherent to any electrical system and specifically to the electrified transit systems. This interference must be well evaluated to enable proper operation of the sub-system components, which are normally designed to achieve a predetermined level of immunity. The interdependence between the EMI emitters and potential victim sub-systems is governed by the well-recognized and widely applied EMC standards, such as EN 50121 or IEC 62236, and their applicable references. These standards define and impose the EM emissions and susceptibility limits for a variety of possible electromagnetic phenomena but leave open an issue of voltages induced on a variety of system wires.

Transit systems are particularly sensitive when it comes to electromagnetic (EM) phenomena because they contain a variety of signal wires that run long distances along both the traction supply lines and, quite frequently, the HV power lines capable of generating large, short circuit currents and inducing destructive or dangerous touch potentials. Another specificity of a traction system is a frequent need to run power cables and signal wires within the same duct bank with minimum lateral separation, which may lead to high levels of induced voltages, especially during shorts and overloads that may occur in the power circuits.

The Vancouver SkyTrain is a major electrified transit system servicing the suburbs and the city center. Its latest extension along Broadway Corridor from Great Northern Way to Arbutus Street includes traction power substations (TPSS) feeding Utility Centers (UC) located over 2 km away from the feed point. Those feeds include medium voltage power cables with short circuit capacity in an order of 20 to 30 kA. Most of the system being underground, the cables are run in the tunnel, in a cable tray in proximity to a signal cable tray. Under such conditions, EMC compatibility requires that the assessment of the impact of power cables on signal wires be done to guide the low power system immunity design. The power cables were originally scheduled at 1.4 m away from the signal tray in a tight side by side configuration and only 40 cm away from the system ground. Calculation based on the formulas derived in this paper revealed that a phase-to-

phase short does not induce any significant voltage in the signaling system wires, however, any short circuit to ground would induce voltages of up to 760 V, providing unsafe and dangerous conditions for personnel and electronics.

High frequency applications installed within the area of the modern transit systems, such as high-power inductive power chargers must be run at a safe distance from the signaling wires. At currently used frequencies in a range of 85 kHz and currents as high as several hundred amperes, even the short runs of signal wires in the proximity of such devices causes a risk due to common mode voltages that may couple to electronics causing breakdown or malfunction. Separation of 20 cm in those circumstances will result in voltage values of about 40 V per the noisy-pair's running meter.

To properly mitigate the effects of the induced voltage in signal wires and shields, it is first necessary to assess their time-value characteristics.

Induced voltage prediction methods

Many authors attempted to model the interaction between the noise-source and victim wires. Moine et.al [1] attempted to calculate an interaction between the HV line and signals using the multi-conductor transmission line (MTL) method presented in [2]. The method is based on the assessment of the impedance matrix involving all HV line phases and a signal wire as shown in [3]. A much different approach is presented in [4], however, the analysis relates to the magnetic field generated by a lightning-related transient in a HV line. There, the authors use harmonic analysis to compose the induced voltage in a victim conductor – a pipeline. In [5], the author proposes to analyze the induced voltages by defining the electric and magnetic fields in the vicinity of the above-ground pipeline and based on that, establishing the sectional mutual impedance.

Most of the available research papers studying Electromagnetic Interference in the form of the induced voltage, result from the need to understand the impact of long runs of the high voltage transmission lines on buried structures laid over long distances in parallel to those lines or on the ground wires protecting the High Voltage Lines from high potentials of highly charged clouds. The calculation

methods use predominantly the mutual impedance approach, while the method of calculating the impedance may vary. A typical example of such an approach is [6-7] where the authors calculate electrostatically and inductively induced ground wire voltages to optimize their sectionalization.

Another practical research trend includes predicting the induced voltages due to lightning currents. Some of those papers, e.g. [8], present the experimental studies and measurements of an impact both the lightning and equipment switching transients have on signal wires.

Yet another important area of research on induced voltages comes from the low power electronics applications using very high frequency signals in various neighboring traces laid near one another within a small area of the printed circuit board, as in [9].

Authors of [10-12] deal with noise in transit system signal wires resulting from power harmonics in the short circuit of the third rail to ground by determining the mutual inductance between the source and victim circuits. There, the mutual inductance is derived based on current mirroring and its soil resistivity-based distribution.

This paper attempts to provide a computing methodology to calculate the induced voltages in the rail transit systems low-voltage and signal wires, which are routinely run over long distances in conduits within the duct banks containing power cables carrying high frequency harmonics. The derived analytical formulas for the induced voltage are confirmed by first reducing the general case of a signal wire run arbitrarily to a noisy pair to two simplified cases, and then comparing the numerical calculations with the results obtained from the Maxwell-software-based electromagnetic simulations.

Simplification

It is important to note that the formulas in this paper are derived for the non-conductive, magnetically homogenous environment for both the source and the victim and that the electric current is contained in an infinitely thin wire. Under those assumptions, calculations done for the air medium are the most conservative, yielding the highest voltages, and once the electromagnetic compliance is proven under those assumptions, no further calculations need to be run.

Magnetic Vector Potential

The two Maxwell equations for the magnetic field can be written as follows:

$$(1) \quad \nabla \times \left(\frac{1}{\mu} \mathbf{B} \right) = \mathbf{J} + \epsilon_0 \frac{\partial \mathbf{E}}{\partial t}$$

$$(2) \quad \nabla \cdot \mathbf{B} = 0$$

Equation (2) implies that $\mathbf{B} = \nabla \times \mathbf{A}$ as $\nabla \cdot (\nabla \times \mathbf{A}) = 0$, always. For low frequency fields the value of $\epsilon_0 \frac{\partial \mathbf{E}}{\partial t}$ in (1) becomes negligible and because $\frac{1}{\mu}$ is constant in the homogenous medium, then it commutes with the differential operator leading to the following equation: $\nabla \times (\nabla \times \mathbf{A}) = \mu \mathbf{J}$. Making use of vector identity: $\nabla \times (\nabla \times \mathbf{A}) = \nabla \cdot (\nabla \cdot \mathbf{A}) - (\nabla \cdot \nabla) \mathbf{A}$ and imposing the Coulomb gauge $\nabla \cdot \mathbf{A} = 0$, the following is achieved: $\nabla^2 \mathbf{A} = -\mu \mathbf{J}$, which can be interpreted as three Poisson scalar equations. The equation can be solved with the help of the Green's Function rendering the following:

$$(3) \quad \mathbf{A}(\mathbf{r}) = \frac{\mu}{4\pi} \iiint \frac{\mathbf{J}(\mathbf{r}')}{d} dV'$$

Where distance $d = |\mathbf{r} - \mathbf{r}'|$ and vectors \mathbf{r} and \mathbf{r}' signify the result point and the source point respectively.

Magnetic Vector Potential for wires

For currents flowing in wires: $\mathbf{J}(\mathbf{r}') dV' = \mathbf{J}(\mathbf{r}') dS \cdot d\mathbf{l} = I(\mathbf{r}') \cdot d\mathbf{l}$, which leads to the following:

$$(4) \quad \mathbf{A}(\mathbf{r}) = \frac{\mu}{4\pi} \int \frac{I(\mathbf{r}')}{|\mathbf{r} - \mathbf{r}'|} d\mathbf{l}'$$

Assuming that the source wires are straight and infinite, the Magnetic vector potential will have a direction of the source current. If the positive source current, I , aligns with the z-axis, the Magnetic vector potential of an arbitrary point P_0 , defined by vector \mathbf{r} , is given as: $\mathbf{A}(\mathbf{r}) = \overrightarrow{A_P} = A_P \overrightarrow{1_z}$. Assuming d_1 to be a distance from the source current to point P_0 and following equation (4), we achieve:

$$(5) \quad A_P = \frac{\mu_0}{4\pi} \int_{-\infty}^{\infty} \frac{I dz}{\sqrt{d_1^2 + z^2}} = \frac{\mu_0}{4\pi} \lim_{\Gamma \rightarrow \infty} \int_{-\Gamma}^{\Gamma} \frac{I dz}{\sqrt{d_1^2 + z^2}}$$

$$(6) \quad A_P = \frac{\mu_0}{2\pi} \lim_{\Gamma \rightarrow \infty} \int_0^{\Gamma} \frac{I dz}{\sqrt{d_1^2 + z^2}} = \lim_{\Gamma \rightarrow \infty} \frac{\mu_0 I}{2\pi} \ln \left(\frac{\Gamma}{d_1} + \sqrt{1 + \frac{\Gamma^2}{d_1^2}} \right)$$

For finite but large values of Γ ($\Gamma \gg d_1$) (6) converts to:

$A_P = \frac{\mu_0 I}{2\pi} \left(-\ln \frac{d_1}{\Gamma} + \ln \frac{2\Gamma}{d_1} \right)$ which helps to avoid unbounded value of the vector potential due to the previously assumed infinite length of the wire.

If the current returns to the source by a parallel return wire or parallel system ground wire, d_2 -distance away from point P_0 , the vector potential at point P_0 becomes a sum of the vector potential generated by each wire:

$A_{P_0} = \frac{\mu_0 I}{2\pi} \left(-\ln \frac{d_1}{\Gamma} + \ln \frac{2\Gamma}{d_1} \right) + \frac{\mu_0 (-I)}{2\pi} \left(-\ln \frac{d_2}{\Gamma} + \ln \frac{2\Gamma}{d_r} \right)$ leading to:

$$(7) \quad A_{P_0} = \frac{\mu_0 I}{2\pi} \left(-\ln \frac{d_1}{d_r} + \ln \frac{d_2}{d_r} \right) = \frac{\mu_0 I}{2\pi} \ln \frac{d_2}{d_1}$$

As can be seen from (7), for a pair of parallel wires, there is no uncertainty in the solution for the vector potential despite an infinite length of the source wires.

In general, a signal wire, further referred to as a "victim", affected by a pair of source wires (noisy wires) can be positioned at any arbitrary distance and angle with respect to the noisy pair. However, among the number of relative positions there are two distinct ones that are often found within the duct banks. One, where the victim wire runs in parallel to a noisy pair and another where a victim runs in a plane perpendicular to the plane created by a noisy pair.

Voltage induced in a victim wire parallel to a noisy pair

Assuming, as mentioned above, that the noisy source wire aligns with the z-axis of the XYZ co-ordinate system, the parallel return wire can be positioned in the YZ plane at a known distance d_w , thus anchoring the source wires. The parallel-victim-wire's position can then be described by a pair of co-ordinates (x_0, y_0) , as shown in Figure 1.

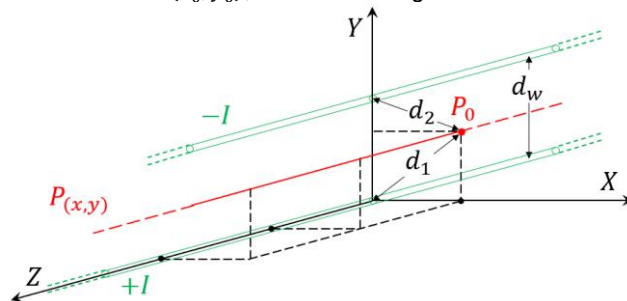


Fig. 1. Relative position of the noisy pair and a victim wire

With the positional metrics of d_w and (x_0, y_0) , (7) can be written as: $A_{P_0} = \frac{\mu_0 I}{2\pi} \ln \frac{\sqrt{(d_w - y_0)^2 + x_0^2}}{\sqrt{x_0^2 + y_0^2}}$, where $d_1 = \sqrt{x_0^2 + y_0^2}$ and

$d_2 = \sqrt{(d_w - y_0)^2 + x_0^2}$. Now, combining $\mathbf{B} = \nabla \times \mathbf{A}$ with the Faraday's equation $\nabla \times \mathbf{E} = -\frac{\partial \mathbf{B}}{\partial t}$ and assuming absence of static charge, the following is achieved: $E_P = -\frac{\partial A_{P_0}}{\partial t}$. Since the wires are stationary, the only time varying component of A_{P_0} is current, $I = I_1 \sin \omega_1 t$, where $\omega_1 = 2\pi f_1$, the electric field amplitude $E_{P_0 V_{max}}$ at point P_0 as well as any other point $P(x, y)$ on the victim wire can be calculated as follows:

$$E_{P_0 V_{max}} = -\frac{\mu_0}{2\pi} \ln \frac{\sqrt{(d_w - y_0)^2 + x_0^2}}{\sqrt{x_0^2 + y_0^2}} \frac{\partial I}{\partial t} = -\frac{\mu_0 I_1 \omega_1}{2\pi} \ln \frac{\sqrt{(d_w - y_0)^2 + x_0^2}}{\sqrt{x_0^2 + y_0^2}} = -\mu_0 f_1 I_1 \ln \frac{\sqrt{(d_w - y_0)^2 + x_0^2}}{\sqrt{x_0^2 + y_0^2}} = -\mu_0 f_1 I_1 \ln \frac{d_2}{d_1}$$

To calculate the induced voltage, an integral of $-\mathbf{E}$ -field along the victim wire must be calculated. Since the wire's increment $dl = dz$, if the run of the victim wire is L , then voltage on this section of the wire can be calculated as:

$$U_{max} = \int_{-L/2}^{L/2} -(-\mu_0 f_1 I_1 \ln \frac{d_2}{d_1}) \cdot dl = L \mu_0 f_1 I_1 \ln \frac{d_2}{d_1} \text{ or:}$$

$$(8) \quad U_{max} = L \mu_0 f_1 I_1 \ln \frac{\sqrt{(d_w - y_0)^2 + x_0^2}}{\sqrt{x_0^2 + y_0^2}} = 2\pi L f_1 A_{P_0, max}$$

A case of victim wire in a plane perpendicular to a YZ plane defined by a noisy source pair

It is very often a case that the victim wire runs in plane perpendicular to the plane containing the source wires. The source wires are placed as before, with the positive current flowing in a wire coinciding with the z-axis of the XYZ coordinate system and the return wire parallel and in YZ plane, as depicted in Figure 2.

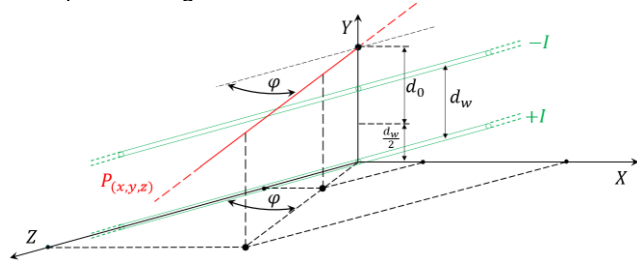


Fig. 2. Victim wire in a plane vertical to a source wires plane

If point $P(x, y, z)$ is a point on the victim wire, the Magnetic vector potential in P points in a direction of z-axis and can be written as $\mathbf{A}(\mathbf{r}) = \overline{A_P} = A_P \overline{1_z}$, where $A_P = \frac{\mu_0 I}{2\pi} \ln \frac{d_2}{d_1}$ and where distances d_1 and d_2 from P to the noisy pair's bottom and top wires are $d_1 = \sqrt{(d_0 + \frac{d_w}{2})^2 + (z \cdot \tan \varphi)^2}$ and $d_2 = \sqrt{(d_0 - \frac{d_w}{2})^2 + (z \cdot \tan \varphi)^2}$, respectively, and where d_w is a distance between the source wires, d_0 a distance from the mid-point between the source wires and the plain containing a victim wire, and φ is an angle between the z-axis and the projection of the victim wire on a ZX plane. Substituting respective distances into $\overline{A_P}$ we achieve:

$$(9) \quad \overline{A_P} = \overline{1_z} \cdot \frac{\mu_0 I}{2\pi} \ln \frac{\sqrt{(d_0 - \frac{d_w}{2})^2 + (z \cdot \tan \varphi)^2}}{\sqrt{(d_0 + \frac{d_w}{2})^2 + (z \cdot \tan \varphi)^2}}$$

The component of the vector potential along the victim wire depends on φ as follows:

$$(10) \quad A_P(z) = \frac{\mu_0 I}{2\pi} \cos \varphi \ln \frac{\sqrt{(d_0 - \frac{d_w}{2})^2 + (z \cdot \tan \varphi)^2}}{\sqrt{(d_0 + \frac{d_w}{2})^2 + (z \cdot \tan \varphi)^2}}$$

$$\text{Where } A_{P, max} = \frac{\mu_0 I_1}{2\pi} \cos \varphi \ln \frac{\sqrt{(d_0 - \frac{d_w}{2})^2 + (z \cdot \tan \varphi)^2}}{\sqrt{(d_0 + \frac{d_w}{2})^2 + (z \cdot \tan \varphi)^2}}$$

Consequently, the maximum electric field along the victim wire is a function of z-coordinate of point P , and equals:

$$(11) \quad E_{max}(z) = -\frac{\partial A_P}{\partial t} = -\mu_0 f_1 I_1 \cos \varphi \ln \frac{\sqrt{(d_0 - \frac{d_w}{2})^2 + (z \cdot \tan \varphi)^2}}{\sqrt{(d_0 + \frac{d_w}{2})^2 + (z \cdot \tan \varphi)^2}}$$

To calculate the voltage induced in the section of the victim wire between two points, $P_A(x, y, z_A)$ and $P_B(x, y, z_B)$, integration of the electric field must be done along the length of the wire from P_A to P_B . To do so, one must notice that the increment dl along the length of the victim wire equals to $\frac{dz}{\cos \varphi}$. Now, the integration can be done in z domain as follows:

$$(12) \quad U_{max} = \int_{z_A}^{z_B} \mu_0 f_1 I_1 \cos \varphi \ln \frac{\sqrt{(d_0 - \frac{d_w}{2})^2 + (z \cdot \tan \varphi)^2}}{\sqrt{(d_0 + \frac{d_w}{2})^2 + (z \cdot \tan \varphi)^2}} \cdot \frac{dz}{\cos \varphi} = \int_{z_A}^{z_B} \frac{2\pi f_1}{\cos \varphi} A_{P, max} \cdot dz$$

The integration can easily be done digitally using a trapezoidal integration method and any computational software including such an easily accessible tool as Microsoft Excel. Dividing the computational domain (z_A, z_B) into n segments and assuming $z_0 = z_A$ and $z_n = z_B$ converts the integral into the following formula for digital applications:

$$(13) \quad U_{max} = 0.5 \cdot \sum_1^n \mu_0 f_1 I_1 \ln \left(\frac{\sqrt{(d_0 - \frac{d_w}{2})^2 + (z_n \cdot \tan \varphi)^2}}{\sqrt{(d_0 + \frac{d_w}{2})^2 + (z_n \cdot \tan \varphi)^2}} \cdot \frac{\sqrt{(d_0 - \frac{d_w}{2})^2 + (z_{n-1} \cdot \tan \varphi)^2}}{\sqrt{(d_0 + \frac{d_w}{2})^2 + (z_{n-1} \cdot \tan \varphi)^2}} \right) \cdot \frac{z_B - z_A}{n}$$

The victim wire positioned at an arbitrary angle to a noisy pair – general case

Figure 3 shows the victim wire positioned at an arbitrary angle to the noisy source wires. The position of the victim wire is anchored by selecting a pair of points, $P_0(0, y_0, 0)$ and $P_1(x_1, 0, z_1)$, that define a new $X'Y'Z$ co-ordinate system with the noisy pair in an $Y'Z$ plane.

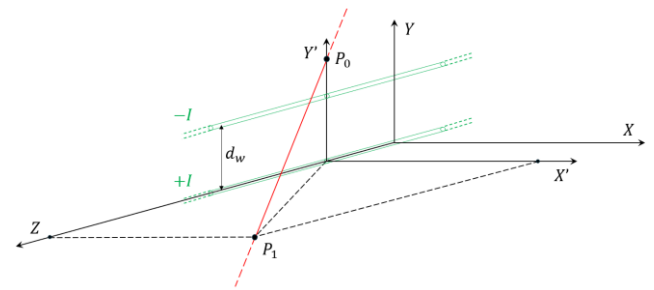


Fig. 3. Victim wire at an arbitrary angle to a noisy pair

The distances between an arbitrary point $P(x', y', z)$ and the respective top and bottom noisy wires are given as:

$$(14) \quad d_1 = \sqrt{(x')^2 + (y')^2}$$

$$(15) \quad d_2 = \sqrt{(x')^2 + (y' - d_w)^2}$$

resulting in the following vector potential at P :

$$(16) \quad \vec{A}_P = \vec{1}_z \cdot \frac{\mu_0 I}{2\pi} \ln \frac{\sqrt{(x')^2 + (y' - d_w)^2}}{\sqrt{(x')^2 + (y')^2}}$$

To calculate the induced voltage, E -field integration must be performed along the length of the victim wire. To facilitate this, the vector potential in P must be converted into a z -variable function. With reference to Figure 3, it can be noticed that x' and y' co-ordinates of point $P(x', y', z)$ relate to z -coordinate as follows: $x' = z \cdot \frac{x_1}{z_1}$ and $y' = y_0 \left(1 - \frac{z}{z_1}\right)$. Substituting for x' and y' in (14) and (15), the distances from the noisy wires to P calculate as:

$$(17) \quad d_1 = \sqrt{\left(\frac{x_1}{z_1} \cdot z\right)^2 + y_0^2 \left(1 - \frac{z}{z_1}\right)^2}$$

$$(18) \quad d_2 = \sqrt{\left(\frac{x_1}{z_1} \cdot z\right)^2 + \left(y_0 \left(1 - \frac{z}{z_1}\right) - d_w\right)^2}$$

Finally, substituting d_1 and d_2 into (16) results in:

$$(19) \quad \vec{A}_P = \vec{1}_z \cdot \frac{\mu_0 I}{2\pi} \ln \frac{\sqrt{\left(\frac{x_1}{z_1} z\right)^2 + \left(y_0 \left(1 - \frac{z}{z_1}\right) - d_w\right)^2}}{\sqrt{\left(\frac{x_1}{z_1} z\right)^2 + y_0^2 \left(1 - \frac{z}{z_1}\right)^2}}$$

Making the \vec{A}_P a function of z .

Once again, with reference to Figure 3, it can be noticed that the component of the vector potential in a victim-wire-direction (the projection of \vec{A}_P onto the victim wire) is a product of $|\vec{A}_P|$ and cosine of the angle between the z -axis and the victim wire, which equals $\frac{z_1}{\sqrt{x_1^2 + y_0^2 + z_1^2}}$. The resultant

value of the victim wire's vector potential, A_{PV} , can now be expressed in z as follows:

$$(20) \quad A_{PV} = \frac{\mu_0 I}{2\pi} \cdot \frac{z_1}{\sqrt{x_1^2 + y_0^2 + z_1^2}} \cdot \ln \frac{\sqrt{\left(\frac{x_1}{z_1} z\right)^2 + \left(y_0 \left(1 - \frac{z}{z_1}\right) - d_w\right)^2}}{\sqrt{\left(\frac{x_1}{z_1} z\right)^2 + y_0^2 \left(1 - \frac{z}{z_1}\right)^2}}$$

$$\text{Where } A_{PV_{max}} = \frac{\mu_0 I_1}{2\pi} \cdot \frac{z_1}{\sqrt{x_1^2 + y_0^2 + z_1^2}} \cdot \ln \frac{\sqrt{\left(\frac{x_1}{z_1} z\right)^2 + \left(y_0 \left(1 - \frac{z}{z_1}\right) - d_w\right)^2}}{\sqrt{\left(\frac{x_1}{z_1} z\right)^2 + y_0^2 \left(1 - \frac{z}{z_1}\right)^2}}$$

Consequently, the maximum electric field, $E_{PV_{max}}$, along the victim wire, caused by a time varying sinusoidal current I of frequency f_1 and amplitude I_1 , calculates as:

$$(21) \quad E_{PV_{max}} = -\frac{\partial A_{PV}}{\partial t} = -\mu_0 f_1 I_1 \cdot \frac{z_1}{\sqrt{x_1^2 + y_0^2 + z_1^2}} \cdot \ln \frac{\sqrt{\left(\frac{x_1}{z_1} z\right)^2 + \left(y_0 \left(1 - \frac{z}{z_1}\right) - d_w\right)^2}}{\sqrt{\left(\frac{x_1}{z_1} z\right)^2 + y_0^2 \left(1 - \frac{z}{z_1}\right)^2}}$$

To calculate the voltage induced in the section of the victim wire between two points, $P_A(x', y', z_A)$ and $P_B(x', y', z_B)$, integration of the electric field must be done along the length of the wire from P_A to P_B . To do so, one must notice that the increment dl along the length of the victim wire

relates to dz as follows $dl = \frac{z_1}{\sqrt{x_1^2 + y_0^2 + z_1^2}} dz$. Now, as in the previous case, the integration can be done in z domain:

$$(22) \quad U_{max} = \int_{z_A}^{z_B} \mu_0 f_1 I_1 \frac{z_1}{\sqrt{x_1^2 + y_0^2 + z_1^2}} \cdot \ln \frac{\sqrt{\left(\frac{x_1}{z_1} z\right)^2 + \left(y_0 \left(1 - \frac{z}{z_1}\right) - d_w\right)^2}}{\sqrt{\left(\frac{x_1}{z_1} z\right)^2 + y_0^2 \left(1 - \frac{z}{z_1}\right)^2}} \cdot \frac{z_1}{\sqrt{x_1^2 + y_0^2 + z_1^2}} dz = \int_{z_A}^{z_B} \mu_0 f_1 I_1 \ln \frac{\sqrt{\left(\frac{x_1}{z_1} z\right)^2 + \left(y_0 \left(1 - \frac{z}{z_1}\right) - d_w\right)^2}}{\sqrt{\left(\frac{x_1}{z_1} z\right)^2 + y_0^2 \left(1 - \frac{z}{z_1}\right)^2}} dz = \int_{z_A}^{z_B} 2\pi f_1 A_{PV_{max}} \frac{z_1}{\sqrt{x_1^2 + y_0^2 + z_1^2}} dz$$

As in the previous chapter, the integration can be done digitally using a trapezoidal integration method. Dividing the computational domain (z_A, z_B) into n segments and assuming $z_0 = z_A$ and $z_n = z_B$ converts the integral into the following formula for digital applications:

$$(23) \quad U_{max} = 0.5 \cdot \sum_{i=1}^n \mu_0 f_1 I_1 \ln \left(\frac{\sqrt{\left(\frac{x_1}{z_1} \cdot z_n\right)^2 + \left(y_0 \left(1 - \frac{z_n}{z_1}\right) - d_w\right)^2}}{\sqrt{\left(\frac{x_1}{z_1} \cdot z_n\right)^2 + y_0^2 \left(1 - \frac{z_n}{z_1}\right)^2}} \cdot \frac{\sqrt{\left(\frac{x_1}{z_1} \cdot z_{n-1}\right)^2 + \left(y_0 \left(1 - \frac{z_{n-1}}{z_1}\right) - d_w\right)^2}}{\sqrt{\left(\frac{x_1}{z_1} \cdot z_{n-1}\right)^2 + y_0^2 \left(1 - \frac{z_{n-1}}{z_1}\right)^2}} \right)^{\frac{z_B - z_A}{n}}$$

Equations proofing

The correctness and consistency of derived formulas can be checked by reducing the **general case** of a victim wire running at an arbitrary angle to a noisy pair, to each of the two simplified cases, one where the victim wire runs in a plane perpendicular to a plain containing the noisy pair and the other where all three wires run in parallel to one another. In the first case, one must observe that the ratio of $\frac{z_1}{z_1}$ from formula (20) is equal $\tan \varphi$ (tangent of angle φ in Figure 2), and that $z_1, x_1 \rightarrow \infty$. What follows is that $\frac{z_1}{\sqrt{x_1^2 + y_0^2 + z_1^2}} = \cos \varphi$.

This is because $\frac{z_1}{\sqrt{x_1^2 + y_0^2 + z_1^2}} = \frac{1}{\sqrt{\frac{x_1^2}{z_1^2} + 1}} = \frac{1}{\sqrt{(\tan \varphi)^2 + 1}}$. Further, with

reference to Figure 3 and Figure 2, $y_0 - d_w = d_0 - \frac{d_w}{2}$ and $y_0 = d_0 + \frac{d_w}{2}$. Considering the above, (20) simplifies to (10).

To simplify the general case to the simplest case of a victim wire running in parallel to a noisy pair at distances d_1, d_2 , the following observations are made based on Figure 3: firstly, as z_1 tends to infinity, the ratio of $\frac{z_1}{z_1}$ tends to zero, modifying both the numerator and the denominator of an argument under the logarithm of (20), which become $y_0 - d_w$ and y_0 , respectively. Secondly, it must be observed that $y_0 = d_1$ and $y_0 - d_w = d_2$ which simplifies (20) to (7), and a general case simplifies to a simple case.

Analytics and Maxwell simulation results

To validate the induced voltage equations, comparison of the analytical and simulation results was done for all three analyzed cases using the Maxwell electromagnetics simulation tool.

Both the simulation and analytical metric parameters are shown in Table 1, where CASE 1 relates to a victim wire run in parallel to a noisy pair; CASE 2 relates to a victim wire run in a plane perpendicular to a plane containing the noisy pair; CASE 3 relates to a victim wire at an arbitrary angle to a noisy pair – a general case.

Table 1. Wire positioning metric

Parameter	CASE 1	CASE 2	CASE 3
d_w [m]	0.5	0.5	0.5
d_0 [m]	n/a	0.35	n/a
φ [rad]	n/a	0.349	n/a
$P_0(x, y, z)$ [m]	(0.2, 0, 0)	n/a	(0, 0.6, 0)
$P_1(x, y, z)$ [m]	n/a	n/a	(10, 0, 27.45)
I_1 [A]	1000	1000	1000
f_1 [Hz]	20,000	20,000	20,000
Z_A [m]*	-5.0	-5.0	-5.0
Z_B [m]*	5.0	5.0	5.0

*NOTE: Z_A and Z_B define integration range: $\int_{Z_A}^{Z_B} f(z) dz$

Table 2. Induced voltage per meter length of victim wire

	CASE 1	CASE 2	CASE 3
<i>Analytics</i> [V]	248.94	-95.48	-95.21
<i>Maxwell</i> [V]	248.64	-95.34	-95.015

It must be noted that the parameters selected for the above comparison do not correlate with a particular practical case and serve the purpose of proving correctness of the derived formulas.

Maxwell CASE 1

Figure 4 shows the vector graph of the vector potential on the line connecting the bottom noisy wire and a victim wire positioned in the XYZ at P_0 as defined in Table 1. The vector lengths captured on that line are maxima that occur at the maximum current. Thus, the minimum value of 0.00019786 Wb/m shown on the legend in the bottom left corner of Figure 4 is the maximum value of the vector potential at the position of the victim wire.

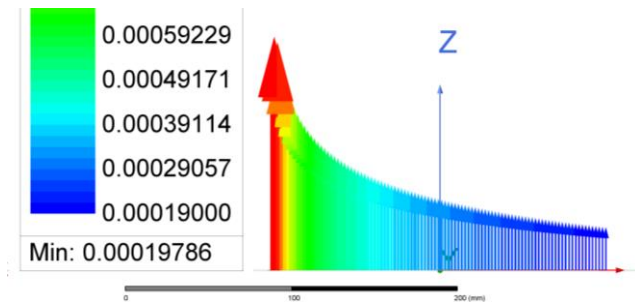


Fig. 4. Vector potential magnitude between the noisy bottom wire and victim wire

Using the simulated result of vector potential and (8), the maximum induced voltage equals: $U_{max} = 2\pi L f_1 A_{P_0,max} = 2\pi \cdot (Z_B - Z_A) f_1 A_{P_0,max} = 248.64 V$, which agrees with the value obtained analytically.

Maxwell CASE 2

In Case 2, the calculation of the induced voltage can be done in 3D, as in the model shown in Figure 5, however, one might observe that the same result can be achieved in a 2D simulation, integrating along the projection of the victim wire on XY . The vector potential value obtained in the simulation must be corrected by $\cos \varphi$ to account for the component along the victim wire, and then by $1/\sin \varphi$ to account for the ratio of the 2D projection and a true length of the victim wire in 3D that results from the assumed integration range $Z_A \rightarrow Z_B$, in z .

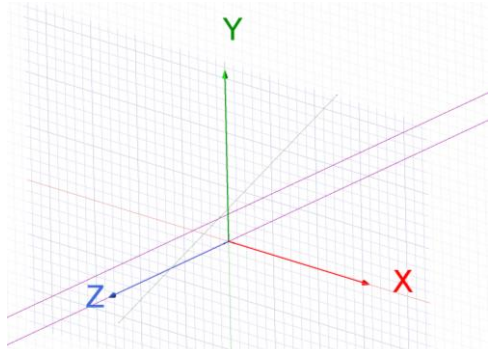


Fig. 5. Victim wire in a plane perpendicular to a plane containing the noisy pair

The distribution of vector potential along the XY projection of the victim wire is shown in Figure 6.

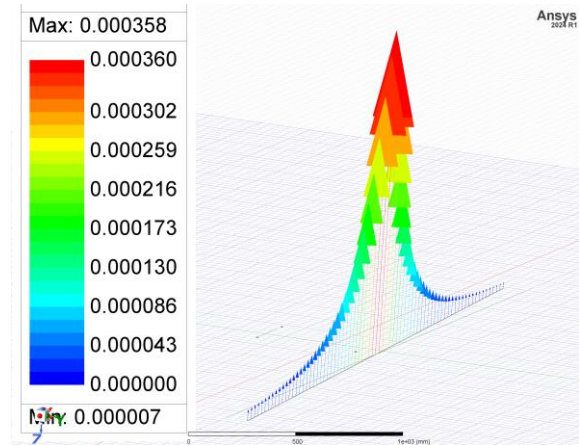


Fig. 6. Distribution of vector potential on an XY projection of the victim wire

Using the simulation results, based on (12), the maximum induced voltage was calculated in a differential calculator provided within the Maxwell software. The simulated voltage value equals: $U_{max} = 95.31 V$, which agrees with the value obtained analytically.

Maxwell CASE 3

Figure 7 shows distribution of the vector potential on an XY projection of the victim wire.

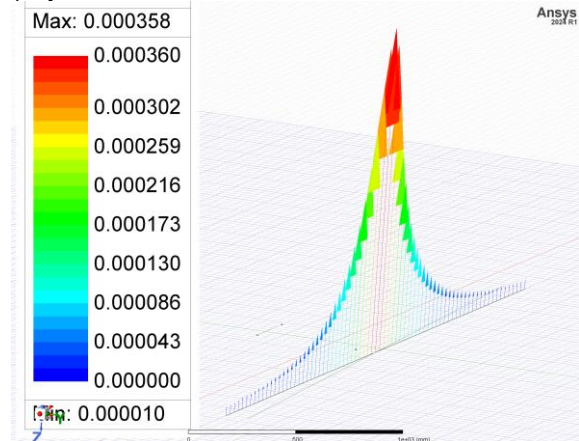


Fig. 7. Distribution of vector potential on an XY projection of the victim wire

In this case, the simulated voltage equals: $U_{max} = 95.015 V$, which agrees with the value obtained analytically.

Two methods were used to prove the formulas. Both the ability to reduce the general case into two simpler cases as well as nearly perfect match between the analytical and the simulation results prove their correctness.

Practical length of the noisy pair

For a given distance $d_2 > d_1$, between the victim wire and a noisy pair, the integration in a range of \pm five times d_2 , ($\Gamma = \pm 5 \cdot d_2$) will always assure 98 % accuracy of the induced voltage. It means that only a part of the noisy pair in an immediate proximity of the victim wire will impact the compatibility outcome and that routing further away from the noisy wire may be neglected.

Conclusions

Induced voltage is an important factor in proving EMC of all electronic systems, and particularly the electric traction systems. The paper provides analytical formulas to calculate the induced voltage in three different most frequently found geometric relations between the noisy wires and the victims – usually the signaling wires. The formulas are double proofed by two different techniques. One, by reducing the general case formula to an intermediate and finally the simplest case, and the second one by comparing the results obtained from the formulas with the results from the electromagnetic simulation software.

More complex cable runs can be easily brought down to one of the three cases described in the paper. In such situations, the ready formulas for the numerical calculations

are presented that can be adapted for a tool of preference including such common tools as MATLAB or Excel.

A real-life example shows the possible magnitudes of the induced voltages, emphasizing the importance of careful assessment of the EMI effects in the systems characterized by extensive use of long, mixed cable runs, such as in electrified traction systems or the systems applying high frequencies.

The formulas are proven and can be used with a high level of confidence by practicing electrical engineers.

Author: D.Sc., Ph.D. Eng. Konrad Woronowicz, West Pomeranian University of Technology, Sikorskiego 37, 70-313 Szczecin, Poland. E-mail: konrad.woronowicz@zut.edu.pl

REFERENCES

- [1] Moine El H., Hassane M., Moussa L., The electromagnetic interference caused by high voltage power lines along the electrical railway equipment, *Int Journal on Elec & Comp Eng*, Vol. 10, No. 5, October 2020: 4581 – 4591
- [2] Adesegun O., *Railway interference management: TLM modelling in railway applications*, Loughborough University, vol. 4, pp. 66-100, 2008
- [3] Minucci S., Pagano M. and Proto D., Model of the 2x25 kV high speed railway supply system taking into account the soil-air interface, *International Journal of Electrical Power and Energy Systems*, vol. 95, pp. 644-652, 201
- [4] Cotton I., Member, IEEE, Kopsidas K., and Zhang Y., Comparison of Transient and Power Frequency-Induced Voltages on a Pipeline Parallel to an Overhead Transmission Line, *IEEE Trans. on Power Delivery*, VOL. 22, NO. 3, JULY 2007
- [5] Ahmed S. AlShahri, Analysis of Induced Potential on Gas/Water Pipelines due to Extra High Voltage AC/DC OHTL, *2022 IEEE 7th International Energy Conference (ENERGYCON) | 978-1-6654-7982-0/22/\$31.00 ©2022 IEEE | doi:10.1109/ENERGYCON53164.2022.9830397*,
- [6] Z. Zhi-Peng, L. Zhen-Qiang, L. Ying and F. Mian, "Study on Overhead Ground Wire Induced Voltage of 500kV AC/DC Transmission Lines for Ice Melting," *2022 7th Asia Conference on Power and Electrical Engineering (ACPEE)*, Hangzhou, China, 2022, pp. 1704-1711, doi: 10.1109/ACPEE53904.2022.9783631
- [7] H. Xiande and Z. Hao, "Simulation and analysis of induced voltage and induced current on overhead ground wire of Jindongnan-Nanyang-Jingmen 1000kV UHV AC transmission line," *2011 4th International Conference on Electric Utility Deregulation and Restructuring and Power Technologies (DRPT)*, Weihai, China, 2011, pp. 622-625, doi: 10.1109/DRPT.2011.5993968.
- [8] Akiyoshi Tatematsu, Kenichi Yamazaki, Kiyotomi Miyajima, and Hideki Motoyama, *Experimental Study of Lightning and Switching Surges-Induced Overvoltages in Low-Voltage Control Circuits*, Proc. of the 2013 International Symposium on Electromagnetic Compatibility (EMC Europe 2013), Brugge, Belgium, September 2-6, 2013
- [9] N. Oka, T. Kumamoto, K. Misu and S. Nitta, "Differential mode noise on the PCB's signal traces converted from external common mode noise," *2009 IEEE International Symposium on Electromagnetic Compatibility*, Austin, TX, USA, 2009, pp. 166-170, doi: 10.1109/ISEMC.2009.5284591.
- [10] L. Yang, L. C. Hian, L. W. Leong and O. M. C. Kevin, "Induced voltage study and measurement for communication system in railway," *2018 IEEE International Symposium on Electromagnetic Compatibility and 2018 IEEE Asia-Pacific Symposium on Electromagnetic Compatibility (EMC/APEMC)*, Suntec City, Singapore, 2018, pp. 32-35, doi: 10.1109/ISEMC.2018.8393733.
- [11] A. Ogunsola and A. Mariscotti, *Electromagnetic Compatibility in Railways Analysis and Management*, Berlin: Springer Berlin, 2014
- [12] W. K. Lo, P. Wong, S. W. Leung, Y. M. Siu and W. N. Sun, "Analysis of induced voltage at close proximity with high voltage cables of electrified railways," *2018 IEEE International Symposium on Electromagnetic Compatibility and 2018 IEEE Asia-Pacific Symposium on Electromagnetic Compatibility (EMC/APEMC)*, Suntec City, Singapore, 2018, pp. 944-947, doi: 10.1109/ISEMC.2018.8393922.